Journal Pre-proof

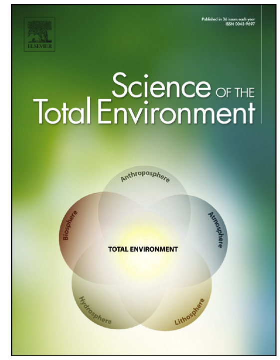

Spatial variability of the green water footprint using a medium-resolution remote sensing technique: The case of soybean production in the Southeast Argentine Pampas

P. Olivera Rodriguez, M.E. Holzman, M.F. Degano, A.M.G. Faramiñán, R.E. Rivas, M.I. Bayala

PII: S0048-9697(20)36493-7

DOI: https://doi.org/10.1016/j.scitotenv.2020.142963

Reference: STOTEN 142963

To appear in: *Science of the Total Environment*

Received date: 8 June 2020

Revised date: 2 October 2020

Accepted date: 6 October 2020

Please cite this article as: P.O. Rodriguez, M.E. Holzman, M.F. Degano, et al., Spatial variability of the green water footprint using a medium- resolution remote sensing technique: The case of soybean production in the Southeast Argentine Pampas, *Science of the Total Environment* (2020), https://doi.org/10.1016/j.scitotenv.2020.142963

Spatial variability of the green water footprint using a medium- resolution remote sensing technique: The case of soybean production in the Southeast Argentine Pampas

P. Olivera Rodriguez a, *, M. E. Holzman a, M. F. Degano b, A. M. G. Faramiñán a, R. E. Rivas b, M. I. Bayala b

a Instituto de Hidrología de Llanuras – Consejo Nacional de Investigaciones Científicas y Técnicas (CONICET)/ Tandil. CP 7000. Buenos Aires, Argentina

b Instituto de Hidrología de Llanuras – Comisión de Investigaciones Científicas (CIC)/ Tandil. CP 7000. Buenos Aires, Argentina

*Corresponding author: polivera@ihlla.org.ar

m.holzman@ihlla.org.ar

mfdegano@ihlla.org.ar

adan.faraminian@ihlla.org.ar

rrivas@rec.unicen.edu.ar

mbayala@ihlla.org.ar

Abstract

Agriculture accounts for about 70% of the fresh water use in the world, dominating rainfed production systems. As meeting future food demand will require an increase in crop production, new techniques are necessary to monitor the spatial variability of agricultural water use. However, the use of remote sensing for the water footprint estimation is limited. This study aims at evaluating the spatial variability of the soil-water consumption in soybean crops, also termed as green water footprint (WF_{green}), in a sector of the Argentine Pampas using satellite data. WF_{green} was evaluated at spatial resolution of 250 m, estimating the soil water availability through the evaporative fraction and crop yield from Moderate-Resolution Imaging Spectroradiometer (MODIS/Aqua) data. In the analysed soybean plots, the WF_{green} varied from 900 m^3 t^{-1} to 1800 m^3 t^{-1}. The preliminary comparison of the method with field measurements showed a RMSE=494 m^3 t^{-1} and Bias=-410 m^3 t^{-1}, respectively. The high spatial variability reflected the heterogeneity of soil-water use efficiency.

The proposed technique can be useful to obtain WF_{green} maps at medium spatial resolutions (250 m - 1000 m). Also, it can be applied in regions with poor ground data coverage to estimate the WF_{green}, after a parameterization of the model. The contribution to our understanding of the relationship between soil-water availability, rainfed-crop productivity and then WF_{green} is expected.

Keywords: Water Footprint, Evaporative fraction, Crop Yield, Efficient agriculture

1. Introduction

According to FAO projections, in order to meet the food demand by 2050, the productivity of existing farmlands needs to increase. This production growth should be accompanied by an efficient use and preservation of natural resources, including water, to prevent future scarcity *(FAO, 2009, 2017; Xinchun et al., 2017)*. Currently, agriculture is responsible for 70% of freshwater use around the world *(FAO, 2016)*, mainly by rainfed crops *(Alexandratos and Bruinsma, 2012; Tadesse et al., 2015)*. Rainfed systems occupy approximately 80% of farmlands and generate 60% of the world food (*IIASA/FAO, 2010; Alvarez et al., 2016*).

In Argentina, only about 15%-20% of the cropland is irrigated. Rainfed systems are dominant in Argentine Pampas (AP) (*Viglizzo et al., 2001; Andrade et al., 2017*), with soybean as the main summer crop (*Viglizzo et al., 2004, Viglizzo and Frank, 2006; Manuel-Navarrete et al., 2014; Ferraro and Gagliostro, 2017).* Argentina produces more than 18% of the world soybean production, being the third world exporter of grains and soy-based products (flour, oil), while 88% of the Argentinean production is generated in the AP *(Ybran and Lacelli, 2016; MAGyP-Argentina, 2018; Bolsa de Comercio de Rosario, 2020)*. The increasing demand for food and fibres has led to the intensification and expansion of soybean production *(Viglizzo and Frank, 2006; Vazquez and Zulaica, 2014)*. There has been a strong pressure on the environment and natural resources, including water resources, limiting their availability for other uses and even competing with the ecological flow *(Ghersa et al., 2002; Vazquez and Zulaica, 2014).* In order to move towards a sustainable crop production, efficient fertilization techniques, conservation tillage practices and efficient use of freshwater resources should be taken into account. Thus, the quantification of the soil-water involved in rainfed crop production and its spatial variability is required to evaluate and optimize its use in such systems *(Galli et al., 2012; Jackson et al., 2015*; *San Luis Agua, 2015; Quinteiro et al.,2019)*.

The water footprint (WF) concept, and particularly the green water footprint (WF_{green}) indicator, is useful to analyse soil-water availability and water use efficiency. The WF is a multidimensional indicator that shows the volumes of water consumed by a product or activity, considering the type of water use: green water or soil water; blue water or surface and groundwater; grey water, or polluted water *(Hoekstra and Hung, 2002; Hoekstra, 2003; Chapagain and Hoekstra, 2004; Hoekstra et al., 2011)*. The WF consists of three components: a) green water footprint (WF_{green}), which represents the rainwater insofar as it does not become run-off and remaining available to the plant use as soil moisture that is exclusively consumed through evapotranspiration process (ET), b) blue water (WF_{blue}), refers to the surface water or groundwater consumed by plant, and c) grey water (WF_{grey}), is the volume of freshwater that is required to assimilate the load of pollutants given natural background concentrations and existing ambient water quality standards *(Hoekstra et al., 2011)*.

Over the last few decades, remote sensing techniques have been suggested to estimate WF *(Romaguera et al., 2010; Toulios et al., 2013; Mekonnen and Hoekstra, 2014; Hoekstra, 2017; Quinteiro et al., 2018)*. The high temporal and spatial coverage of satellite missions can complement the calculation of WF_{green} in regions with poor ground data. Although water productivity, which is calculated as the inverse equation of WF_{green}, has been obtained from remotely sensed data in different studies *(*e.g. *Cai et al., 2009; Bastiaanssen and Steduto, 2017; Amarasinghe and Smakhtin, 2014; de Oliveira Costa et al., 2020)*, the estimation of WF_{green} requires more analysis. *Romaguera et al. (2010)* and *Toulios et al. (2013)* showed the potential of remote sensing to calculate the parameters involved in WF_{green}.

Other studies of WF have contributed to the calculation of ET, but not to the estimation of crop yield (Y). *Romaguera et al. (2010)* proposed a remote sensing model to obtain WF_{green} and WF_{blue} in Egypt, based on mapping irrigated surfaces and soil water balance. Such method incorporates multi-source data and low spatial resolution (10000 m) and simulates continuous data for the entire crop growth cycle from certain crop stages. Also, Y was taken from official statistics. *Romaguera et al. (2012)* proposed a model for green water evapotranspiration (ET_{green}) and blue water evapotranspiration (ET_{blue}) calculation from the Global Land Data Assimilation System (GLDAS). *Karantzalos et al. (2015)* compared empirical methods and the global evapotranspiration product from MODIS (MOD16) for WF_{green} calculation in Vasileia river basin for 4 years over cropland, wood and grassland. However, they did not consider different crop types and their phenology. Also, studies as *Romaguera et al., (2010); Karantzalos et al., (2015); Ortiz, (2016)* proposed the use of the MODIS global evapotranspiration product (MOD16) for ET_{green} calculation. Different authors have reported the low performance of such product, with RMSE about 2-13 mm 8 day^{-1} (0.25-1.63 mm per day) and 4-21 mm 8 day^{-1} (0.50-2.63 mm per day) for actual and potential evapotranspiration, respectively (e.g. *Kim et al., 2012; Autovino et al., 2016; Degano et al., 2018a; 2018b)*.

Data of Y at medium spatial resolution is crucial for the calculation of WF_{green}. Also, given that continuous ground measurements of Y are frequently scarce, different remote sensing methods based on optical and thermal data have been developed (e.g. *Anderson et al., 2016; Holzman and Rivas, 2016; Shrestha et al., 2017; Holzman et al., 2018)*. Recently, the relationship between a water vegetation stress index and Y in AP has been tested, with expected errors about 20% *(Holzman et al., 2014b; Holzman et al., 2018)*.

Another group of studies (e.g. *Siebert and Doll, 2010; Mekonnen and Hoekstra, 2010; Mekonnen and Hoekstra, 2011; Mekonnen and Hoekstra, 2014)* uses the grid method for WF estimation at global scale with a spatial resolution of 10000 m (10000 ha). Input data (rainfall, reference evapotranspiration, soil and crop parameters) to compute ET_{green}, ET_{blue} are obtained from a grid covering the whole world and Y comes from official statistics. Although these studies have pioneered the use of remote sensing for the calculation of the WF, the coarse spatial resolution and the combination of multi-source data with different spatial and temporal resolutions can produce biases derived from data integration *(Bastiaanssen and Steduto, 2017; de Oliveira Costa et al., 2020).* In this context, it is necessary to develop methods with finer spatial resolution and reduced multi-source data.

In this framework, the aim of this study is to assess the spatial estimation of soybean WF_{green} from satellite data in Southeast AP at a spatial resolution of 250 m (~ 6.25 ha).

An alternative approach to the traditional methods that considers the calculation of evaporative fraction (EF) and Y from remotely sensed data is proposed. In addition, this study can be a down-to-earth contribution to the WF calculation of soy-based products consumed around the world, which use imported Argentine soybean as raw materials.

2. Materials and methods

2.1. Study area

The study was carried out in Tandil county, Buenos Aires province, located in the Southeast of AP, covering an area of 4935 km^2 (Fig. 1a). The central area of Buenos Aires province is characterized by a humid-sub humid climate *(Kottek et al., 2006)*. The average annual precipitation is approximately 1000 mm, with sporadic water deficit during December, January and February (which can affect Y of summer crops) and water excess distributed from March to August. The interannual variability determines occasional droughts and floods, producing noticeable Y fluctuations *(Holzman et al., 2014b; Ares et al., 2016; Holzman et al., 2018)*. The average annual temperature is 16 °C and the potential evapotranspiration is about 1200 mm *(Holzman et al., 2014a)*. The main soil order is Mollisol, characterized by a fertile mollic epipedon, high water retention capacity (≈170-220 mm at 0.8 m depth) and good cropping conditions *(GeoINTA, 2020)*. These climatic and soil characteristics have favoured the increase of agricultural activities and the displacement of other uses as livestock *(Viglizzo and Frank, 2006; Vazquez and Zulaica, 2014)*. Currently, agriculture is based on a few rainfed crops, with similar management practices throughout the region, being wheat and soybean the most representative at regional scale *(Ybran and Lacelli, 2016; MAGyP-Argentina, 2018)*.

Field measurements were conducted in a plot ("La Campana", Tandil, 37° 17'S, 58° 56'W, 152 m.a.s.l, Fig. 1b) of 36 ha within the study area. In addition, 8 plots were used to perform in situ WF_{green} estimates (Fig. 1a). In the 9 plots, the soil type corresponds to a Typic Argiudoll with clay loam soil texture *(GeoINTA, 2020)*, covered with soybean crop. The sowing and harvest dates were similar to those recorded in "La Campana" (15/11/2014 and 02/04/2015, respectively), being such dates the characteristic period of soybean crop growth in the region *(Bolsa de Comercio de Rosario, 2020)*. There was no application of fertilizers, due to the previous inoculation of the seed. These plots were chosen because of the field data availability, typical physical characteristics (e.g. soil type, rainfall) and agricultural practices (e.g. fertilization, crops rotation) representative of the study area.

Figure 1. a. Location of Tandil county in Southeast of Argentine Pampas, (Landsat 8-Operational Land Imager, 01/04/2015, RGB 543); b. Soybean plot located in "La Campana", where the energy balance station (EBS_1) was installed for field measurements; c. Energy balance station located on reference cover (EBS_2).

2.2. Field measurement

The calculation of WF_{green} at plot scale was carried out considering the Y data reported in the plots by farmers. The data recorded by two energy balance stations (EBS) of the Instituto de Hidrología de Llanuras and additional data from Tandil Station *(Servicio Meteorológico Nacional Argentino, 2018)* were used. EBS_1 is located in "La Campana" (Fig. 1b), from which only data of NDVI and EF were used. EF calculation in the remaining 8 plots was generated using precipitation data (Pp) recorded in the plots, air temperature (Ta), air relative humidity (RH), wind speed (u) measured by Servicio

Meteorológico Nacional Argentino, Tandil Station (37° 14´S, 59° 15´W, 175 m.a.s.l.) and texture, structure and soil water capacity data obtained from *GeoINTA, (2020)*. EBS_2 is located on a reference surface *(Allen et al., 1998; 2006)* in the campus of the Universidad Nacional del Centro de la Provincia de Buenos Aires (37° 19´S, 59° 05´W, 211 m.a.s.l.) (Fig. 1c). In EBS_2 the daily average values of net radiation (R_n), Ta, RH, u were selected for the estimation of reference evapotranspiration (ET_0). Patm (kPa) data were obtained from Servicio Meteorológico Nacional Argentino, Tandil Station.

The EBS record at 15-minute intervals data of R_n, wind speed, Ta and RH, soil heat flux (G), soil moisture and temperature, land surface temperature (Ts), Normalized Difference Vegetation Index (NDVI), among other variables. R_n was measured by a CNR-1net radiometer (Kipp and Zonen - Netherlands). It records separately the incident and outgoing radiation, both shortwave and longwave, by means of its four components: two CM3 pyranometers (0.305 - 2.800 μm) and two CG3 pyrgeometers (5-50 μm). The CM3 and CG3 sensors have a maximum error of 2.5%. Ta and HR were recorded by the sensor CS215-L16 (Campbell Scientific, Inc.-United States) which has a maximum error of 0.4 °C and 2%, respectively, considering typical ranges of measurement. NDVI was measured by SRS sensors (Decagon Devices, Inc.-United States), positioned vertical to the ground, which have an error of 10% for spectral irradiance and radiance values.

The instruments were mounted on an iron mast 2.60 m above the surface and data were stored in a CR10X datalogger (Campbell Scientific, Inc.-United States). The datalogger was connected to a 12 V battery with a 20 W solar panel for recharging *(Carmona, 2013; Carmona et al., 2011)*. Besides, the EBS_1 has a cylindrical weighing lysimeter with a surface of 0.27 m^2 and 0.85 m depth for EF estimation *(Ocampo et al.,* *2012)*. This is connected to an electronic balance that measures continuously the difference of weight according to the water content in the soil, allowing the calculation of water availability for crop use.

2.3. Methods

According to the methodology proposed by the Water Footprint Manual *(Hoekstra et al., 2011)*, the WF_{green} during the growing period of a crop (m^3 t^{-1}) is calculated as the green component of crop water use (CWU_{green}, m^3 ha^{-1}) divided by the crop yield (Y, t ha^{-1}) (Eq. (1)).

$$WF_{green} = \frac{CWU_{green}}{Y} \tag{1}$$

where CWU_{green} is calculated by accumulating daily green evapotranspiration (ET_{green}, mm day^{-1}) over the complete crop growing period (Eq. (2)).

$$CWU_{green} = 10 \sum_{d=1}^{h} ET_{green} \tag{2}$$

where ET_{green} is the daily green water evapotranspiration and 10 is a conversion factor from mm to m^3 ha^{-1}. The summation is done over the period from the day of planting (d=1) to the day of harvest (d=h).

In this study, daily values of ET_{green} were obtained by quantifying the adjusted crop evapotranspiration (ET_a, mm day^{-1}), that is, the crop evapotranspiration under non-optimal conditions of soil water availability for rainfed soybean (Eq. (3)).

$$ET_{green} = ET_a = K_s\, ET_c \; = \; K_s\, K_c\, ET_o \tag{3}$$

where ET_c (mm day^{-1}) is the crop evapotranspiration, ET_0 (mm day^{-1}) represents the reference evapotranspiration, K_c (dimensionless) is the crop coefficients and K_s

(dimensionless) is the water stress coefficient *(Allen et al., 1998; 2006).* The soil water availability has temporal and spatial variability, which frequently limits crop growth and its subsequent Y. Thus, the use of K_s suggested in *(Hoekstra et al., 2011)* was considered. We assumed that water involved in ET_{green} does not come from groundwater, given that in the study area groundwater level sporadically reaches 1.2 m depth mainly in livestock zones and during autumn and winter, with deeper level during spring and summer *(Verselli et al., 2019)*. Croplands in the study area are associated to higher zones suitable for cropping.

2.3.1. Green crop water use and green water evapotranspiration

2.3.1.1. Reference crop evapotranspiration

Reference crop evapotranspiration (ET_0, mm day^{-1}) was calculated according to the FAO-Penman Monteith method *(Allen et al., 1998; 2006)* (Eq. (4)):

$$ET_0 = \frac{0.408\Delta(R_n - G) + \gamma\frac{900}{Ta+273}u_2(e_s - e_a)}{\Delta + \gamma(1 + 0.34u_2)} \quad (4)$$

where Δ is the slope of the saturation vapour pressure curve as a function of air temperature (kPa °C^{-1}), R_n is net radiation (MJ m^{-2} day^{-1}), G is soil heat flux (MJ m^{-2} day^{-1}), which was considered zero, given that at daily scale and high vegetation cover it is negligible *(Allen et al., 1998; Sánchez et al., 2008)*. γ is the psychrometric constant (kPa °C^{-1}), Ta is the mean daily air temperature at 2-m height (°C), u_2 is wind speed at 2-m height [m s^{-1}], (e_s-e_a) is vapour pressure deficit. 0.408 is a conversion factor to mm day^{-1}, 900 is a coefficient for the reference crop (kJ^{-1} Kg K day^{-1}), 273 is a conversion factor to express the temperature in K and 0.34 is a coefficient resulting from assuming a crop resistance of 70 s m^{-1} and an aerodynamic drag of 208 u^{-2} for the reference crop (s m^{-1}).

ET_0 (Eq. (4)) was calculated daily, using data of R_n, Ta, RH, and wind speed recorded from EBS_2 (Fig. 1c). The obtained ET_0 was considered as representative of the ET_0 at county level, since the atmospheric parameters determining ET_0 do not vary significantly within a radius of around 150 km in a large plain as the study area *(Rivas and Caselles, 2004)*.

2.3.1.2. Crop coefficient

The crop coefficient (K_c) was obtained based on the Normalized Difference Vegetation Index (NDVI) applying the equation suggested by *Kamble et al. (2013)* for soybean and corn, with expected errors about 19% (Eq. (5)):

$$Kc = 1.46\, NDVI - 0.17 \qquad (5)$$

where, NDVI is the NDVI for the considered pixel and was calculated according to *Rouse et al., (1974)* (Eq. (6)).

$$NDVI = \frac{(NIR - R)}{(NIR + R)} \qquad (6)$$

where, NIR represents the surface reflectance in the near-infrared and R the surface reflectance in the red wavebands.

Changes in morphological and physiological characteristics of crop modify K_c values during the growth period. Therefore, K_c was calculated for the typical 4 stages of soybean growth reported in literature *(Allen et al., 2006; Andriani, 2017)*: initial growth stage (25 days), development growth stage (30 days), mid-season growth stage (60 days), end of the late season growth stage (24 days). In the evaluated soybean plot in "La Campana", the daily NDVI values were measured by the SRS sensor in EBS_1. Then, NDVI values (measured at the time of maximum radiation and cloud free) were obtained for each stage and K_c was calculated using the Eq. (5). These K_c values were considered for all the analysed plots, since they have the same crop, similar sowing and harvest dates, and are located within the same climatic and edaphic area. At county scale, NDVI was obtained from the MODIS vegetation indices product MYD13Q1 (see more details in 2.3.1.3). Subsequently, a linear regression was carried out to verify the correlation between the NDVI values recorded by the SRS sensor in the soybean plot and those obtained with the MODIS MYD13Q1 product.

2.3.1.3. Water stress coefficient

The water stress coefficient (K_s) describes the effect of water stress on crop transpiration and was calculated as function of evaporative fraction (EF), considering $EF=K_s$. From the surface energy balance point of view, EF is defined as the relationship between latent heat flux (evapotranspiration) and the available energy at the land surface (latent heat flux+sensible heat flux), being an indicator of the soil moisture availability for vegetation use. Under conditions of high soil moisture, EF tends to 1 and the available energy is used mainly for ET. With scarce or no soil moisture, most of the available energy is allocated to the sensible heat flux and EF approaches zero *(Kurc and Small, 2004; Mallick et al., 2009).*

In the case of “La Campana”, daily EF at soybean plot level was estimated according to *Ocampo et al. (2012)*. This method is based on Eq. (7) using the weighing lysimeter of ESB_1:

$$EF_{wl} = (W_{di} - W_{min})/(W_{max} - W_{min}) \quad (7)$$

where, EF_{wl} (dimensionless) is the lysimeter evaporative fraction, W_{di} is the weight of the weighing lysimeter of a certain day, W_{min} is the minimum weight (264 kg) representing minimum water content in the soil profile (54 mm) and W_{max} is the maximum weight recorded in the lysimeter (312 kg) equivalent to the soil field capacity (227 mm).

The other considered plots do not have a weighing lysimeter. Therefore, the EF was obtained through a soil water balance, using the CROPWAT model.

EF varies according to soil moisture, showing high spatial heterogeneity due to different factors (soil types, texture and structure of soils, among others), resulting in fluctuations of ET_{green}. Therefore, EF at county scale was calculated using optical/thermal data from satellite that allow considering such spatial variability *(Nutini et al., 2014)* (Eq. (8)):

$$EF = 1 - TVDI \quad (8)$$

where TVDI is the Temperature Vegetation Dryness Index, based on the inverse relationship between Ts and vegetation index *(Sandholt et al., 2002)*. Several authors *(*e.g. *Nutini et al., 2014; Carlson and Petropoulos, 2019)* have estimated EF from the triangular scatterplot of Ts in function of NDVI from medium resolution satellite data, with expected errors about 25%. *Holzman et al. (2014a, 2014b)* have shown this index has high correlation (R^2>0.7) with soil water availability for crops in the root zone, which was measured in the study area with the same sensors mentioned in this study. Hence, TVDI was considered as an indicator of soil water availability in ET. This index was calculated as *(Sandholt et al., 2002)* (Eq. (9)):

$$TVDI = (Ts - Ts_{min}) / (a + b\ NDVI - Ts_{min}) \quad (9)$$

where, Ts is the observed surface temperature (K) at a given pixel, Ts_{min} is the minimum surface temperature for a region/image representing maximum soil moisture and evapotranspiration, a+bNDVI represents Ts_{max} (minimum soil moisture and evapotranspiration) while a and b are surface parameters of the study area calculated from the inverse linear relationship between Ts and vegetation index *(Holzman et al., 2014b)*.

TVDI was obtained from MODIS/AQUA data products with a spatial resolution of 250 m: a) MYD11A2: 8-day composite Ts, level-3, version-5, 1 km spatial resolution, using a total of 18 images for the study period, b) MYD13Q1: 16-day composite vegetation index, level-3, version-5, 250 m (9 images). The MYD11A2 product was resampled at 250 m using the nearest neighbour algorithm, to equate spatial resolutions. The images of Ts and NDVI obtained in each month were averaged to generate a monthly TVDI image (Eq. (9)), except in the case of November, where the TVDI product corresponds to the last 16 days of the month. Subsequently, 5 images of EF were generated according to the Eq. (8).

2.3.1.4. Maps of crop plots and green crop water use

A land use classification from multispectral Landsat 8 Operational Land Imager (OLI) was conducted, covering the period of maximum vegetative growth of soybean (04/01/2015). The atmospheric and angular reflectance correction (BDRF) function was applied to the image. Then, the visible, near-infrared (NIR), shortwave-infrared (SWIR) surface reflectance (BOA) was used to perform a supervised classification using 6 different classes, based on the information provided by farmers, which allowed training and evaluating the algorithm accuracy. A land use classification using Spectral Information Divergence method to extract the soybean plots was carried out

(Du et al. 2004). The classification was evaluated statistically with a confusion matrix-based approach, which compared the mapped class with the ground truth data at specific locations. Conventional accuracy statistics (Kappa coefficient, commission, omission and overall accuracies) were then derived from the confusion matrix *(Egorov et al., 2015; Foody, 2002)*. Then a mask of soybean plots was generated and applied to the EF and Y maps. To obtain the maps at the plot level, the mask was upscaled to 250 m using the nearest neighbourhood method *(Bayala and Rivas, 2014; Richards, 1999).*

Using the ground ET_0, and satellite estimations of K_c and K_s (i.e. EF), Eq. (3) was applied in ENVI software to estimate ET_{green}. Due to the changes of the K_c and EF data during the crop growth period, the ET_{green} maps were generated for each stage. Finally, a map of CWU_{green} for the entire crop cycle was generated from the sum of ET_{green} for each stage.

2.3.2. Yield estimation

For plot-scale calculation of WF_{green}, the Y obtained in the plot was used (Eq. (1)). On the other hand, previous studies have shown that TVDI is appropriate to estimate spatially Y *(Holzman et al., 2014b; Holzman and Rivas, 2016; Holzman et al., 2018)*. These studies have analysed Y series from 2000 to 2011, considering dry, normal and humid campaigns in AP. They showed a high correlation (R^2=0.6-0.83) between this index (during critical growth stage of crops) and ground measurements of yield of maize, soybean and wheat at county and plot level. Linear and quadratic adjustments were found depending on crop type and agroclimatic conditions. Therefore, Y at county scale was estimated from TVDI images using the equation proposed by *Holzman et al. (2014b)* with expected errors about 20%:

$$Y = C_1\,(TVDI)^2 + C_2 TVDI + C_3 \quad (10)$$

where TVDI is the monthly index for the critical period of the crop (when crop shows the highest sensitivity to water deficit, coinciding with the flowering period and seed pod development). This period includes January and February for soybean in the study area *(MAGyP-Argentina, 2018)*. C_1, C_2 and C_3 are coefficients that depend on the agro-ecological region derived from the adjustment between observed data of Y and TVDI *(Holzman et al., 2014b; Holzman and Rivas, 2016)*.

Finally, with CWU_{green} and Y data, the WF_{green} was obtained at plot and county scale. The methodological diagram of the study is included in Fig. 2.

2.3.3. Comparison between green water footprint from traditional grid method and the proposed approach

WF_{green} was calculated applying the traditional grid method to later compare results obtained with field measurements and the proposed method (Fig. 2). It was estimated at 10000 m spatial resolution *(Siebert y Doll, 2010; Mekonnen and Hoekstra, 2010)* applying a soil water balance in the grid cells where each of the 9 plots of study area are located.

ET_{green} was calculated for the entire crop growth period following the method proposed by *Allen et al. (1998)* for crops under non-optimal conditions of water availability (Eq. (3)). The FAO CROPWAT *(Allen et al., 1998)* was used with monthly rainfall, minimum and maximum Ta and HR as input data at 10000 m spatial resolution. These data were taken from the CRU TS, version 4 *(Harris et al., 2020).* The K_c, standard crop depletion fraction, rooting depth and the other crop and soil parameters were taken from the Table 2 of *Siebert and Doll (2008)*. The used value of soil water capacity was consistent with the ISRICWISE grid database, which is at 10000 m spatial resolution *(Batjes, 2012)*. The K_s was obtained as result of the simulation from FAO CROPWAT. Y data of soybean crop was taken from official statistics for Tandil County *(MAGyP-Argentina, 2020)*.

Finally, to verify the robustness of the grid and the satellite methods, both datasets were compared with the WF_{green} values derived from in situ measurements. The performance of each method was evaluated using the root mean square error (RMSE) and Bias.

Figure 2. Methodological diagram, which includes the three WF_{green} estimates: local data (orange), the proposed approach based on remote sensing data (blue), and grid method (purple). ET_0 (grey) was obtained from local measurements recorded in ESB_2 and was used as input data for WF_{green} estimates in the soybean plot and at county scale.

3. Results and discussion

3.1. Green water footprint in soybean plot

Fig. 4 shows the evolution of ET_0, K_c, EF and ET_{green} (the last three calculated in "La Campana") during the soybean growth period. In the initial growth stage, there was is scarce vegetation cover (K_c = 0.60), with the evaporation predominating over the transpiration process, therefore the daily values of ET_{green} were are low. In the development crop stage, an increase in ET_{green} was is observed, but the decrease in water availability for the crop at the end of this stage caused a decrease in the ET_{green} values. In the middle growth stage, the plant completed its vegetative and reproductive development (K_c = 1.09) and ET_{green} reached maximum values. The soil water availability was is close to the optimum (EF = 0.93), hence ET_0 approached ET_{green}. During the end growth stage, ET_{green} decreased considerably as a consequence of plant senescence (K_c = 0.64), increasing the difference between ET_0 and ET_{green} despite the availability of water in the soil. The obtained K_c values were consistent with those reported for soybean by *Andriani (2017)*, *Chapagain and Hoekstra (2004)* and *Allen et al. (2006)* for soybean in sub-humid regions. Also, the NDVI measured in the plot showed high correlation with the MODIS MYD13Q1 data (R^2=0.78), with minimum and maximum between 0.13-0.81 and 0.11-0.79, respectively.

Figure 3. ET_0, K_c, EF and ET_{green} values calculated from the planting date to the harvest date of soybean.

The total ET_0 was 602 mm and the total ET_{green} value was 411 mm, resulting in a CWU_{green} of 4110 m^3 ha^{-1} for the entire growth period (Eq. (2)). Considering that the Y measured in “La Campana” plot was equal to 2.5 t ha^{-1}, a value of WF_{green}≈1645 m^3 t^{-1} was obtained. This result is similar to values obtained in other plots analysed in Tandil county (Table 2). Also, these are close to WF_{green} values estimated by other authors as *Ercin et al. (2012)*, who obtained soybean WF_{green} ≈2000 m^3 t^{-1} in two different environments of Canada and France, with Y=2.5 t ha^{-1} and 1.9 t ha^{-1}, respectively. On the other hand, *Costa et al. (2018)* in Western Pará, Amazon, determined a WF_{green}≈1600 m^3 t^{-1} with Y average of 1.9 t ha^{-1} in eight soybean plots. The differences of WF_{green} values may be explained by diverse variables: crop genetics (which affects the water use efficiency), meteorological characteristics of each region, soil type and agricultural management. These variables can influence both Y and

ET_{green}. However, in plots studied in the county the difference would be due to rainfall variability and the geomorphology of the land, which affects the soil water availability, influencing water consumption of plant, as explained in Section 5.2.4.

3.2. Estimation of green water footprint from remotely sensed data

3.2.1. Soybean crop map

In order to calculate ET_{green} at county-scale, plots with soybean crop were classified. Fig. 4 shows the result of the supervised classification obtained through Spectral Information Divergence. Table 1 includes omission or commission errors of the classification, showing a precision or overall accuracy of 78.35%, and a Kappa coefficient of 0.72. Such mask was used to consider only soybean plot for WF_{green} calculation.

Figure 4. a. Land use classification. In green, the plot of soybean for campaign 2014-2015; b. Ground truth map used for classification and number of samples for each class.

Table 1. Confusion matrix of the supervised classification.

3.2.2. Green crop water use map

A noticeable spatial variation of CWU_{green} in Tandil county is shown in Fig. 5.a. It varies approximately between 1800 m^3 ha^{-1} and 3600 m^3 ha^{-1} in most plots, although there are areas where CWU_{green} values are close to 5400 m^3 ha^{-1}. These areas coincide with the presence of two types of soils whose characteristics could favour higher ET_{green} *(GeoINTA, 2020)*:

- In the South and Centre of the county, the soils are productive but shallow, thus the evapotranspiration process prevails upon the infiltration process.

- In the Northwest and East area, soils are deep and developed, suitable for agricultural production. The permeability and slow runoff facilitate the rainfall retention and water storage (EF with values close to 1).

5.2.3. Spatial calculation of yield

As a previous step to WF_{green} calculation, Y was estimated spatially for the analysed campaign (Fig. 5.b). Eq. (10) was applied considering the following coefficients for the study area: C_1=0 (due to a lineal relationship between Y and TVDI), C_2= -1990.1 and C_3=4260.5 *(Holzman et al. 2014b)*. These parameters vary for different large regions. However, once the model is calibrated with ground data of Y that include the maximum expected variability, it can be used for spatial estimation of Y. Fig. 5.b shows that Y was between 1.5 t ha^{-1} and 3 t ha^{-1} in most of cases. A group of plots with high Y (3 t ha^{-1}) is observed in areas where the maximum values of CWU_{green} were obtained, which corresponds to high soil water availability and more productive soils with the consequent positive impact on Y (e.g. high organic matter content, strong vertical development).

Figure 5. a. Green crop water use (CWU_{green}) in soybean plots; b. Map of soybean crop yield estimated from MODIS data in Tandil county during the campaign 2014/2015.

5.2.4. Green water footprint map

As shown in Fig. 6, the proposed method can reflect the spatial heterogeneity of factors determining the WF_{green}, with most values varying between 900 m^3 t^{-1} and 1800 m^3 t^{-1}. The distribution of plots with low WF_{green} volume coincides with the sites where Y is high. Therefore, low WF_{green} volume would be related to the existence of more productive soils *(GeoINTA, 2020)*.

Figure 6. Spatial distribution of green water footprint (WF_{green}) values in Tandil county obtained from MODIS data at 250 m spatial resolution.

In the Northeast and East of the county, plots with high WF_{green} values are concentrated, as a result of low Y. However, plots with high WF_{green} values were found all over the county. The inability to translate CWU_{green} into higher productivity could be due to the existence of limiting factors, such as the presence of limestone material or rock, clayey horizons, poor soil drainage and topography relief that modify the water storage capacity of rainfall water in the soil, as well the root development. Hence, they can affect the availability of water for crop use, producing different CWU_{green} and Y in each plot.

In the South and Northwest of the county, the WF_{green} values were also close to the maximum, in spite of high Y, which is related to high values of CWU_{green} (Fig. 5.a)

In recent years, the demand for soybean and the grain market has encouraged the expansion of the land used for crop production. Livestock, which plays a key role in some areas of the county with poorer soils, has been displaced *(Ghersa et al., 2002; Viglizzo and Frank, 2006; Vazquez and Zulaica, 2014)*. Consequently, plots with limitations for agricultural activity were cultivated, which currently can generate these high WF_{green} values and low water productivity. Also, the spatial heterogeneity of WF_{green} is associated with the distribution of rainfall and the topographic and morphological characteristics of the study area. Although in this study the agricultural practices in the county have not been evaluated, they could explain certain spatial changes in WF_{green}. Management practices related to the preservation of soil moisture content can influence the Y.

A WF_{green} mean value of 1350 m^3 t^{-1} for Tandil county was obtained, which was close to the 1290 m^3 t^{-1} average value obtained by *Aldaya et al. (2010)* for soybean crops in Argentina. However, the difference is markedly greater if we consider the volume of WF_{green} calculated by *Mekonnen and Hoekstra (2011)* for rainfed soybean crops in Argentina (2079 m^3 t^{-1}), using the grid method. This difference can be related to the plot area and the low spatial resolution (10000 m) of the grid method. The sub-pixel heterogeneity con influence the estimation of WF_{green}. Such difference also could be related to the multi-source data of Y. It seems that the implementation of a higher spatial resolution could increase the precision of the method, being a contribution for estimation of water involved in agricultural production. In this study we consider that a spatial resolution of 250 m is suitable for the study area, with extensive agriculture and most of the plots with a surface of 100 ha.

The use of the Mapping Evapotranspiration at High Resolution Internalized Calibration (METRIC) model has also been previously considered for the spatial estimation of ET_{green} at a scale of 30 m, from LANDSAT data *(Allen et al., 2007)*. This model has shown a good performance estimating the ET of various crops *(Choi et al., 2009; Singh et al., 2012; Paço, et al., 2014; de Oliveira Costa et al., 2020)*. It is methodologically similar to our proposed method to obtain ET_{green}, but the analysis scale is different. LANDSAT data offer a higher spatial resolution, justifying its use at the plot level, but they have a lower temporal resolution. The existence of cloudiness and the narrow swaths make it difficult to apply in large areas. Medium resolution satellites like MODIS provide a suitable temporal coverage to monitor crop changes during the growth stage with appropriate spatial resolution at regional or landscape scales. Therefore, the size of the AP plots justifies the use of MODIS, with a spatial resolution of 250 m. Also, the expectable low sub-pixel heterogeneity due to the existence of few crops as in the study area would produce reliable results.

Finally, a preliminary comparison of the results obtained from the proposed satellite method and the grid method with field measurements was carried out (Table 2). The RMSE values suggested a better performance of the satellite method than the grid method. A significant trend to overestimate WF_{green} was observed in the grid method, with a Bias=575 m^3 t^{-1}. On the other hand, the proposed method underestimate the WF_{green}. It should be noted that the grid method uses mean data of Y and parameters of CWU for a wide area (e.g. county), which are useful for studies at regional or country scale, but can affect the precision of the method at plot scale *(Romaguera et al. 2010)*. As mentioned, there are several factors affecting soil water availability and consequently crop yield. In this sense, the proposed method considers the spatial and temporal heterogeneity od CWU and Y, which can contribute to the estimation of WF_{green}.

Table 2. Comparison between the traditional grid method, field measurements and the proposed approach based on satellite data.

Conclusions

This study proposes a remote sensing technique for the spatial estimation of WF_{green} at 250 m spatial resolution. The variables required for the WF_{green} calculation (i.e. CWU, Y) were estimated from MODIS/Aqua data, with minimum field measurements requirements. EF and Y are the main input variables of the method.

The maps of WF_{green} for soybean crop estimated by the proposed technique in Tandil county of Argentine Pampas varied from 900 m^3 t^{-1} to 1800 m^3 t^{-1}. These values are consistent with studies carried out in Argentina and other regions of the world such as Canada, USA, France and Brazil *(Aldaya et al., 2010; Ercin et al., 2012; Costa et al., 2018)*. In order to evaluate the obtained results, the WF_{green} was also estimated on soybean plots using local data and using the grid method. This preliminary comparison suggested a better performance of the proposed method (RMSE=494 m^3 t^{-1}) in comparison with the grid method (RMSE= 597 m^3 t^{-1}), with a trend to overestimate WF_{green}.

The study identifies sites where the high volumes of soil-water involved in the evapotranspiration process produce high Y and sites where WF_{green} increases, in which improvements of water use efficiency would be necessary.

The complexity of method for spatial calculation of WF_{green} resides mainly in the calibration of Y equation and evaporative fraction estimation, whose coefficients are the results of a simple regional parameterization. Despite this, essential data such as ET_0 or NDVI, are easily accessible and can be considered from multiple databases, facilitating the applicability of this technique in other regions of the world. The proposed approach can contribute to the efficient crop production and could be applied on other crops and highly productive regions with limited ground data as Sub-Saharan Africa and Chinese Great Plains.

Acknowledgements

The authors would like to acknowledge Consejo Nacional de Investigaciones Científicas y Técnicas and the Instituto de Hidrología de Llanuras for supporting part of this research. We also appreciate to traders and farm workers that kindly accepted to participate in the study.

References

Aldaya, M. M., Allan, J. A., Hoekstra, A. Y. (2010). Strategic importance of green water in international crop trade. Ecol. Indic. 69 (4), 887-894. http://ageconsearch.umn.edu/record/136934

Alexandratos, N., Bruinsma, J. (2012). World Agriculture Towards 2030/2050: The 2012 Revision. ESA Working Paper No 12-30. Rome. http://www.fao.org/docrep/016/ap106e/ap106e.pdf

Allen, R. G., Pereira, L. S., Raes, D., Smith, M. (1998). Crop evapotranspiration: guidelines for computing crop water requirements. FAO Irrigation and Drainage 56, Rome, Italy. http://www.climasouth.eu/sites/dault/files/FAO%2056.pdf

Allen, R.G., Pereira, L.S., Raes, D., Smith, M. (2006). Evapotranspiración del cultivo. Guías para la determinación de los requisitos de agua de los cultivos. Riego y Drenaje de la FAO, 56. Roma, Italia. http://www.fao.org/3/x0490s/x0490s.pdf

Allen, R. G., Tasumi, M., Trezza, R. (2007). Satellite-based energy balance for mapping evapotranspiration with internalized calibration (METRIC)—Model. J. Irrig. Drain. Eng. 133(4), 380-394.https://doi.org/10.1061/(ASCE)0733-9437(2007)133:4(380)

Alvarez, A., Morábito, J. A., Schilardi, C. (2016). "Huellas hídricas verde y azul del cultivo de maíz (Zea mayz) en provincias del centro y noreste argentino". Rev. Fac. Cienc. Agrar., Univ. Nac. Cuyo 48(1), 161-177. http://www.scielo.org.ar/scielo.php?script=sci_arttext&pid=S1853-86652016000100012&lng=es&nrm=iso

Amarasinghe, U. A., Smakhtin, V. (2014). Water productivity and water footprint: misguided concepts or useful tools in water management and policy?. Water Int. 39(7), 1000-1017. https://doi.org/10.1080/02508060.2015.986631

Anderson, M.C., Zolin, C.A., Sentelhas, P.C., Hain, C.R., Semmens, K., Yilmaz, M.T., Gao, F., Otkin, J.A., Tetrault, R., (2016). The Evaporative Stress Index as an indicator of agricultural drought in Brazil: An assessment based on crop yield impacts. Remote Sens. Environ. 174, 82-99. https://doi.org/10.1016/j.rse.2015.11.034

Andrade, F., Taboada, M., Lema, D., Maceira, N., Echeverría, H., Posse, G., Gamundi, J. C. (2017). Los desafíos de la agricultura argentina. Ciudad Autónoma de Buenos Aires, Argentina: Ediciones INTA. http://repositorio.inta.gob.ar/handle/20.500.12123/2149

Andriani, J. M. (2017). Coeficientes de cultivos para los principales cultivos extensivos de la Región Pampeana. http://hdl.handle.net/20.500.12123/1922

Anschau, R. A., Bongiovanni, R., Tuninetti, L., Manazza, F., Mercedes, R. V. (2015). Huella hídrica de la cadena de maní en Argentina. Avances y estado de situación en análisis de ciclo de vida y huellas ambientales en la Argentina (Water footprint of the peanut chain in Argentina. Progress and status in life cycle analysis and environmental footprints in Argentina). IV Encuentro Argentino de Ciclo de Vida y III Encuentro de la Red Argentina de Huella Hídrica ENARCIV. November 5 to 6, Cordoba, Argentina. http://refhub.elsevier.com/S0959-6526(18)30919-3/sref4

Ares, M. G., Bongiorno, F., Holzman, M., Chagas, C., Varni, M., Entraigas, I. (2016). Water erosion and connectivity analysis during a year with high precipitations in a watershed of Argentina. Hydrol. Res. 47(6), 1239-1252. https://doi.org/https://doi.org/10.2166/nh.2016.179

Autovino, D., Minacapilli, M., Provenzano, G. (2016). "Modelling bulk surface resistance by MODIS data and assessment of MOD16A2 evapotranspiration product in an irrigation district of Southern Italy". Agric. Water Manage. 167, 86-94. https://doi.org/10.1016/j.agwat.2016.01.006

Bastiaanssen, W. G., Steduto, P. (2017). The water productivity score (WPS) at global and regional level: Methodology and first results from remote sensing measurements of wheat, rice and maize. Sci. Total Environ. 575, 595-611. https://doi.org/10.1016/j.scitotenv.2016.09.032

Batjes, N. H. (2012). ISRIC-WISE derived soil properties on a 5 by 5 arc-minutes global grid (ver. 1.2) (No. 2012/01). ISRIC-World Soil Information. https://library.wur.nl/WebQuery/wurpubs/fulltext/206736

Bayala, M. I., Rivas, R. E. (2014). Enhanced sharpening procedures on edge difference and water stress index basis over heterogeneous landscape of sub-humid region. Egypt. J. Remote Sens. Space Sci. 17(1), 17-27. https://doi.org/10.1016/j.ejrs.2014.05.002

Bolsa de Comercio de Rosario, (2020). Informe de Estimación Mensual Nacional. Available online: https://bcr.com.ar/es [Accessed April 20, 2020].

Cai, X., Thenkabail, P. S., Biradar, C. M., Platonov, A., Gumma, M., Dheeravath, V., Cohen, Y., Goldshleger, N., Ben-Dor, E., Alchanatis, V., Markandu, A., Vithanage, J. (2009). Water productivity mapping using remote sensing data of various resolutions to support. J. Appl. Remote Sens. 3(1), 033557. https://hdl.handle.net/10568/40587

Carlson, T.N., Petropoulos, G.P. (2019). A new method for estimating of evapotranspiration and surface soil moisture from optical and thermal infrared measurements: the simplified triangle. Int. J. Remote Sens. 4, 7716–7729. https://doi.org/10.1080/01431161.2019.1601288

Carmona, F. (2013). Desarrollo de un modelo general para la estimación de la radiación neta con imágenes de satélite. Tesis Doctoral. Facultad de Física, Departamento de Física de la Tierra y Termodinámica. Universidad de Valencia. [Inédita].
https://core.ac.uk/reader/71020976

Carmona, F., Rivas R., Ocampo D., Schirmbeck J., Holzman M. (2011). “Sensores para la medición y validación de variables hidrológicas a escalas local y regional a partir del balance de energía”. Published in 2010 by the International Hydrological Programme (IHP) of the United Nations Educational, Scientific and Cultural Organization (UNESCO). 3(1), 26–36
http://cursosihlla.bdh.org.ar/ET_Local_Regional_2014/Clase_3/3_Material_Lectura/AquaLAC-Numero1-Vol3.pdf#page=32

Chapagain A. K., Hoekstra, A. Y. (2004). Water footprints of nations. Value of Water Research Report Series No. 16, UNESCO-IHE, Delft, The Netherlands.
http://refhub.elsevier.com/S0921-8009(13)00217-6/rf0040

Choi, M., Kustas, W. P., Anderson, M. C., Allen, R. G., Li, F., Kjaersgaard, J. H. (2009). An intercomparison of three remote sensing-based surface energy balance algorithms over a corn and soybean production region (Iowa, US) during SMACEX. Agric. For. Meteorol. 149(12), 2082-2097.
https://doi.org/10.1016/j.agrformet.2009.07.002

Costa, D. C., Martorano, L. G., Lisboa, L. S. S., Stolf, R. (2018). "Temporal dynamics of the water footprint of soybean hub grains in Western Pará, Amazon". Rev. Ambient. Água 13(5), 1-10. http://dx.doi.org/10.4136/ambi-agua.2051

Degano, M. F., Rivas, R. E., Carmona, F., Faramiñán A., Olivera Rodríguez, P. (2018). Calibración del producto de evapotranspiración potencial "MOD16_A2" para la Región Pampeana Argentina. XIV Congreso Latinoamericano de Hidrogeología. X Congreso Argentino de Hidrogeología. VIII Hispano-latinoamericano sobre temas actuales de la hidrología. October, 23 to 26, Salta, Argentina. https://www.researchgate.net/profile/Ricardo_Sanchez-Murillo/publication/332120201

Degano, M. F., Rivas, R. E., Sánchez, J. M., Carmona, F., Niclòs, R. (2019). Assessment of the Potential Evapotranspiration MODIS Product Using Ground Measurements in the Pampas - IEEE, ARGENCON - 6 al 8 de Junio, 2018, San Miguel de Tucumán, Tucumán, Argentina. http://dx.doi.org/10.1109/ARGENCON.2018.8646143

del Milagro Jorrat, M., Araujo, P. Z., Mele, F. D. (2018). "Sugarcane water footprint in the province of Tucumán, Argentina. Comparison between different management practices". J. Clean. Prod. 188, 521-529. https://doi.org/10.1016/j.jclepro.2018.03.242

de Oliveira Costa, J., José, J. V., Wolff, W., de Oliveira, N. P. R., Oliveira, R. C., Ribeiro, N. L., Schlichting, A. F. (2020). Spatial variability quantification of maize water consumption based on Google EEflux tool. Agric. Water Manage. 232, 106037. https://doi.org/10.1016/j.agwat.2020.106037

Du, Y., Chang, C. I., Ren, H., Chang, C. C., Jensen, J. O., D'Amico, F. M. (2004). New hyperspectral discrimination measure for spectral characterization. Opt. Eng. 43(8), 1777-1787. https://doi.org/10.1117/1.1766301

Egorov, A. V., Hansen, M. C., Roy, D. P., Kommareddy, A., Potapov, P. V. (2015). Image interpretation-guided supervised classification using nested segmentation. Remote Sens. Environ. 165, 135-147. https://doi.org/10.1016/j.rse.2015.04.022

Ercin, A. E., Aldaya, M. M., Hoekstra, A. Y. (2012). "The water footprint of soy milk and soy burger and equivalent animal products". Ecol. Indic. 18, 392-402. https://doi.org/10.1016/j.ecolind.2011.12.009

FAO. 2009. High Level Expert Forum–How to Feed the World in 2050. Available online: http://www.fao.org/fileadmin/templates/wsfs/docs/Issues_papers/HLEF2050_Global_Agriculture.pdf. [Accessed November 29, 2018]

FAO, 2016. AQUASTAT. Food and Agriculture Organization of the United Nations. Available online: http://www.fao.org/nr/water/aquastat/About_us/indexesp.stm [Accessed December 2, 2018]

FAO, 2017. The future of food and agriculture – Trends and challenges. Rome.

Ferraro, D. O., Gagliostro, M. (2017). "Trade-off assessments between environmental and economic indicators in cropping systems of Pampa region (Argentina)". Ecol. Indic. 83, 328-337. https://doi.org/10.1016/j.ecolind.2017.08.020

Foody, G. M. (2002). Status of land cover classification accuracy assessment. Remote Sens. Environ. 80(1), 185-201. https://doi.org/10.1016/S0034-4257(01)00295-4

Galli, A., Wiedmann, T., Ercin, E., Knoblauch, D., Ewing, B., Giljum, S. (2012). "Integrating ecological, carbon and water footprint into a "footprint family" of indicators: definition and role in tracking human pressure on the planet". Ecol. Indic. 16, 100-112. https://doi.org/10.1016/j.ecolind.2011.06.017

Ghersa, C.M., Ferraro, D.O., Omacini, M., Martínez- Ghersa, M.A., Perelman, S., Satorre, E., Soriano, A. (2002). Farm and landscape level variables as indicators of sustainable land use in the Argentine Inland Pampa. Agric. Ecosyst. Environ. 93, 279-293. https://doi.org/10.1016/S0167-8809(01)00351-6

INTA (2020). GeoINTA. Cartas de suelos de la Provincia de Buenos Aires, Argentina. www.visor.geointa.inta.gob.ar. [Accessed February 11, 2020]

Harris, I., Osborn, T. J., Jones, P., Lister, D. (2020). Version 4 of the CRU TS monthly high-resolution gridded multivariate climate dataset. Sci. Data *7*(1), 1-18. https://doi.org/10.1038/s41597-020-0453-3

Hoekstra, A.Y., 2003. "Virtual Water: An Introduction". Virtual Water Trade. Proceedings of the International Expert Meeting on Virtual Water Trade. Values of Water Research Report Series No 12. IHE, Delft, Holland. http://6.worldwaterforum.org/fileadmin/wwc/Programs/Virtual_Water/VirtualWater_Proceedings_IHE.pdf#page=13

Hoekstra, A. Y., Chapagain, A. K., Aldaya, M. M., Mekonnen, M. M. (2009). Water Footprint Manual. State of the Art, 1-131. https://www.narcis.nl/publication/RecordID/oai:ris.utwente.nl:publications%2Fd2aabede-4a7a-49af-be57-17440829ccfd

Hoekstra, A.Y., Chapagain, A.K., Aldaya M.M., Mekonnen M.M. (2011). The Water Footprint Assessment Manual: Setting the global standard. Earthscan, London. http://refhub.elsevier.com/S0959-6526(18)30919-3/sref19

Hoekstra, A. Y., Hung, P. Q. (2002). Virtual water trade: A quantification of virtual water flows between nations in relation to international crop trade. Value of Water

Research Report Series No 11. UNESCO-IHE. https://library.wur.nl/WebQuery/titel/1755106

Holzman, M. E., Rivas, R. (2016). "Early maize yield forecasting from remotely sensed temperature/vegetation index measurements". IEEE J. Sel. Top. Appl. Earth Obs. Remote Sens. 9(1), 507-519. https://doi.org/10.1109/JSTARS.2015.2504262

Holzman, M.E., Rivas, R., Bayala, M. (2014a). "Subsurface soil moisture estimation by VI-LST method". IEEE Geosci. Remote. Sens. Lett. 11(11), 1951-1955. https://doi.org/10.1109/LGRS.2014.2314617

Holzman, M.E., Rivas, R., Piccolo, M.C. (2014b). "Estimating soil moisture and the relationship with crop yield using surface temperature and vegetation index". Int. J. Appl. Earth Obs. Geoinf. 28, 181-192. https://doi.org/10.1016/j.jag.2013.12.006

Holzman, M.E., Carmona, F., Rivas, R., Niclós, R. (2018). "Early assessment of crop yield from remotely sensed water stress and solar radiation data". ISPRS J. Photogramm. Remote Sens. 145, 297–308.https://doi.org/10.1016/j.isprsjprs.2018.03.014

IIASA/FAO. 2010. Global agro-ecological zones (GAEZ v3.0). Laxenburg, Austria, IIASA y Roma, FAO. http://pure.iiasa.ac.at/id/eprint/13290/1/GAEZ_Model_Documentation.pdf

Jackson, N., Konar, M., Hoekstra, A. Y. (2015). The water footprint of food aid. Sustainability, 7(6), 6435-6456. https://doi.org/10.3390/su7066435

Kamble, B., Kilic, A., Hubbard, K. (2013). Estimating crop coefficients using remote sensing-based vegetation index. Remote Sens. 5(4), 1588-1602. https://doi.org/10.3390/rs5041588

Kim, H. W., Hwang, K., Mu, Q., Lee, S. O., Choi, M. (2012). "Validation of MODIS 16 global terrestrial evapotranspiration products in various climates and land cover types in Asia". KSCE J. Civ. Eng. 16(2), 229-238. http://dx.doi.org/10.1007%2Fs12205-012-0006-1

Kottek, M., Grieser, J., Beck, C., Rudolf, B., Rubel, F. (2006). World map of the Köppen-Geiger climate classification updated. Meteorol. Z. 15(3), 259-263. https://doi.org/10.1127/0941-2948/2006/0130

Kurc, S.A., Small, E.E. (2004). "Dynamics of evapotranspiration in semiarid grassland and shrubland ecosystems during the summer monsoon season, central New Mexico". Water Resour. Res. 40, 1–15. https://doi.org/10.1029/2004WR003068

Mallick, K., Bhattacharya, B.K., Patel, N.K. (2009). "Estimating volumetric surface moisture content for cropped soils using a soil wetness index based on surface temperature and NDVI". Agric. For. Meteorol. 149, 1327–1342. https://doi.org/10.1016/j.agrformet.2009.03.004

Manuel-Navarrete, D., Gallopín, G. C., Blanco, M., Díaz-Zorita, M., Ferraro, D. O., Herzer, H., Satorre, E. H. (2009). "Multi-causal and integrated assessment of sustainability: the case of agriculturization in the Argentine Pampas". Environ. Dev. Sustain. 11(3), 621-638. https://doi.org/10.1007/s10668-007-9133-0

Mekonnen, M. M., Hoekstra, A. Y. (2010). "A global and high-resolution assessment of the green, blue and grey water footprint of wheat". Hydrol. Earth Syst. Sci. 14(7), 1259-1276. https://doi.org/10.5194/hess-14-1259-2010

Mekonnen, M. M., Hoekstra, A. Y. (2011). "The green, blue and grey water footprint of crops and derived crop products". Hydrol. Earth Syst. Sci. 15, 1577-1600. https://doi.org/10.5194/hess-15-1577-2011

Mekonnen, M. M., Hoekstra, A. Y. (2014). "Water footprint benchmarks for crop production: A first global assessment". Ecol. Indic. 46, 214-223. https://doi.org/10.1016/j.ecolind.2014.06.013

Nutini, F., Boschetti, M., Candiani, G., Bocchi, S., Brivio, P. (2014). Evaporative fraction as an indicator of moisture condition and water stress status in semi-arid rangeland ecosystems. Remote Sens. 6, 6300–6323. https://doi.org/10.3390/rs6076300

Ocampo, D., Rivas, R. (2011). "Evaluación de métodos de estimación de la evapotranspiración a escala mensual y anual en Argentina: Aplicación en zonas húmedas y áridas". Cuadernos del Curiham, 17, 33-41. http://hdl.handle.net/2133/7161

Ocampo, D., Rivas, R. E., Silicani, M. R., Carmona, F., Holzman, M., Mancino, C. A. (2012). Estimación de la fracción evaporativa a partir de registros de humedad de suelo y un lisímetro de pesada. Encuentro del "International Center For Earth Sciences"-E-ICES 8. October 30 to November 2, Mar del Plata, Buenos Aires, Argentina. http://digital.cic.gba.gob.ar/handle/11746/2353

Oficina de Riesgo Agropecuario-MAGyP-Argentina, 2018. Available online: http://www.ora.gob.ar/ [Accessed June 28, 2018]

Ortiz, C. M. R. (2016). Análisis de la disponibilidad de agua verde a partir del ajuste del cálculo de la evapotranspiración en zonas de vegetación natural. Master's Thesis, Facultad de Minas, Departamento de Geociencias y Medio Ambiente. Universidad Nacional de Colombia. http://www.bdigital.unal.edu.co/53836/

Paço, T. A., Pôças, I., Cunha, M., Silvestre, J. C., Santos, F. L., Paredes, P., Pereira, L. S. (2014). Evapotranspiration and crop coefficients for a super intensive olive orchard. An application of SIMDualKc and METRIC models using ground and satellite observations. J. Hydrol. 519, 2067-2080. https://doi.org/10.1016/j.jhydrol.2014.09.075

Quinteiro, P., Rafael, S., Villanueva-Rey, P., Ridoutt, B., Lopes, M., Arroja, L., Dias, A. C. (2018). "A characterisation model to address the environmental impact of green water flows for water scarcity footprints". Sci. Total Environ. 626, 1210-1218. https://doi.org/10.1016/j.scitotenv.2018.01.201

Quinteiro, P., Rafael, S., Vicente, B., Marta-Almeida, M., Rocha, A., Arroja, L., & Dias, A. C. (2019). Mapping green water scarcity under climate change: A case study of Portugal. Sci. Total Environ. 696, 134024. https://doi.org/10.1016/j.scitotenv.2019.134024

Richards, J. A. (1999). Remote sensing digital image analysis. Springer-Verlag. Berlin.

Rivas, R., Caselles, V. (2004). "A simplified equation to estimate spatial reference evaporation from remote sensing-based surface temperature and local meteorological data". Remote Sens. Environ. 93(1-2), 68-76.https://doi.org/10.1016/j.rse.2004.06.021

Romaguera, M., Hoekstra, A. Y., Su, Z., Krol, M. S., Salama, M. S. (2010). "Potential of using remote sensing techniques for global assessment of water footprint of crops". Remote Sens. 2(4), 1177-1196. https://doi.org/10.3390/rs2041177

Romaguera, M., Salama, M. S., Krol, M. S., Su, Z., Hoekstra, A. Y. (2012). Remote sensing method for estimating green and blue water footprint. Remote Sensing and Hydrology. Proceedings of a symposium. September 27 to 30, Jackson Hole, Wyoming, USA.https://research.utwente.nl/en/publications/remote-sensing-method-for-estimating-green-and-blue-water-footpri

Rouse Jr, J. W., Haas, R. H., Deering, D. W., Schell, J. A., Harlan, J. C. (1974). Monitoring the Vernal Advancement and Retrogradation (Green Wave Effect) of Natural Vegetation. [Great Plains Corridor]. https://ntrs.nasa.gov/search.jsp?R=19750020419

Sánchez, J., Scavone, G., Caselles, V., Valor, E., Copertino, V., Telesca, V. (2008). "Monitoring daily evapotranspiration at a regional scale from Landsat-TM and ETM+ data: Application to the Basilicata region". J. Hydrol. 351, 58-70. https://doi.org/10.1016/j.jhydrol.2007.11.041

Sandholt, I., Rasmussen, K., Andersen, J. (2002). A simple interpretation of the surface temperature/vegetation index space for the assessment of surface moisture stress. Remote Sens. Environ. 79, 213–224. https://doi.org/10.1016/S0034-4257(01)00274-7

San Luis Agua, S. E. (2015). Ministerio del Campo. Gobierno de la Provincia de San Luis. 2014. Cálculo y análisis de la huella hídrica de la Provincia de San Luis. Sectores agrícola y pecuario. Available online: http://www.huellahidrica.org/Reports/Calculo%20Huella%20Hidrica.pdf. [Accessed November 29, 2018]

Servicio Meteorológico Nacional Argentino (2018). Available online: www.smn.gob.ar. [Accessed July 12, 2017]

Shrestha, R., Di, L., Eugene, G. Y., Kang, L., SHAO, Y. Z., BAI, Y. Q. (2017). Regression model to estimate flood impact on corn yield using MODIS NDVI and USDA cropland data layer. J. Integr. Agric. 16(2), 398-407. https://doi.org/10.1016/S2095-3119(16)61502-2

Siebert, S., Doll, P. (2008). The global crop water model (GCWM). Frankfurt Hydrology Paper, 2007, 4-42. https://www.uni-frankfurt.de/45217788/FHP_07_Siebert_and_Doell_2008.pdf

Siebert, S., Döll, P. (2010). Quantifying blue and green virtual water contents in global crop production as well as potential production losses without irrigation. J. Hydrol. 384(3-4), 198-217. https://doi.org/10.1016/j.jhydrol.2009.07.031

Singh, R. K., Liu, S., Tieszen, L. L., Suyker, A. E., Verma, S. B. (2012). Estimating seasonal evapotranspiration from temporal satellite images. Irrig. Sci. 30(4), 303-313. https://doi.org/10.1007/s00271-011-0287-z

Subsecretaria de Mercado Agropecuario-MAGyP-Argentina, 2018. Available online: http://www.magyp.gov.ar/ [Accessed January 17, 2020]

Tadesse, T., Senay, G.B., Berhan, G., Regassa, T., Beyene, S. (2015). “Evaluating a satellite-based seasonal evapotranspiration product and identifying its relationship with other satellite-derived products and crop yield: a case study for Ethiopia”. Int. J. Appl. Earth Obs. Geoinf. 40, 39–54. https://doi.org/10.1016/j.jag.2015.03.006

Tampouratzi, L.V., Papadopoulou, M.P, Karantzalos, K. (2015). Remote sensing and empirical methodologies to assess green water footprint in river basin scale. 14th International Conference on Environmental Science and Technology (CEST). September 3 to 5, Rhodes, Greece. https://www.researchgate.net/publication/284157478_Remote_Sensing_and_Empirical_Methodologies_to_Assess_Green_Water_Footprint_In_River_Basin_Scale

Toulios, L., Romaguera, M., Calleja, E., Stancalie, G., Nertan, A. Struzik, P., Dalla Marta, A., Zoltan, D., Nunes, R., Vuolo, F. (2013). Potential of remote sensing techniques to improve the agriculture water footprint assessment and the virtual water trade accounting. Proceedings of SPIE 8795, First International Conference on Remote Sensing and Geoinformation of the Environment (RSCy2013), August 9, Paphos, Cyprus. https://doi.org/10.1117/12.2027568

Vazquez, P. and L. Zulaica, 2014. Agriculturization and environmental impacts in a representative area of the ecoregion of the Pampas, Argentina. Brazilian Geographical Journal: Geosciences and Humanities research medium 5(1), 20-45. http://hdl.handle.net/11336/25628

Vercelli, N., Varni, M., Lara, B., Entraigas, I. (2019). Linking soil water balance with flood spatial arrangement in an extremely flat landscape. Hydrol. Process. 1–12. https://doi.org/10.1002/hyp.13567

Viglizzo, E. F., Frank, F. C. (2006). Land-use options for Del Plata Basin in South America: Tradeoffs analysis based on ecosystem service provision. Ecol. Econ. 57(1), 140-151. https://doi.org/10.1016/j.ecolecon.2005.03.025

Viglizzo, E. F., Lértora, F., Pordomingo, A. J., Bernardos, J. N., Roberto, Z. E., Del Valle, H. (2001). Ecological lessons and applications from one century of low external-input farming in the pampas of Argentina. Agric. Ecosyst. Environ. 83(1-2), 65-81. https://doi.org/10.1016/S0167-8809(00)00155-9

Viglizzo, E. F., Pordomingo, A. J., Castro, M. G., Lértora, F. A., Bernardos, J. N. (2004). Scale-dependent controls on ecological functions in agroecosystems of Argentina. Agric. Ecosyst. Environ. 101(1), 39-51. https://doi.org/10.1016/S0167-8809(03)00229-9

Xinchun, C., Mengyang, W., Xiangping, G., Yalian, Z., Yan, G., Nan, W., & Weiguang, W. (2017). Assessing water scarcity in agricultural production system based on the generalized water resources and water footprint framework. Sci. Total Environ. 609, 587-597. https://doi.org/10.1016/j.scitotenv.2017.07.191

Ybran, R., Lacelli, A. (2016). Informe estadístico mercado de soja. Instituto Nacional de Tecnología Agropecuario (INTA). Available online: https://inta.gob.ar/sites/default/files/inta_informe_estadistico_del_mercado_de_soja.pdf [Accessed October 27, 2018]

Table 1. Confusion matrix of the supervised classification.

		Ground Truth						Commission	Omission
Class	**Soybean**	**Bare**	**Hill soil**	**Water**	**Woods**	**Urban**	**Total**		
		(Pixels)	**(Pixels)**	**(Pixels)**	**(Pixels)**	**(Pixels)**	**(Pixels)**	**(Pixels)**	**(Pixels)**
Unclassified	0	0	0	139	0	25	164		
Soybean	526	0	0	0	27	0	553	27/553	92/618
Bare	0	368	0	0	1	19	387	19/387	0/368
Hill soil	0	0	59	15	32	132	206	147/206	0/59
Water	0	0	0	45	0	0	45	0/45	155/200
Woods	92	0	0	1	64	6	163	99/163	27/91
Urban	0	0	0	0	0	589	589	0/589	182/771
Total	618	368	59	200	91	771	2107		

Overall Accuracy = (1651/2107) 78.35%

Kappa Coefficient = 0.72

910 Table 2. Comparison between the traditional grid method, field measurements and
911 the proposed approach based on satellite data.

Plots	Method						Analysis period
	Field measurements		Grid method		Satellite data method		
	WF_{green} [a]	Spatial Resolution	WF_{green} [b]	Spatial Resolution	WF_{green} [c]	Spatial Resolution	
	(m^3 t^{-1})		(m^3 t^{-1})	(m)	(m^3 t^{-1})	(m)	(day)
Plot 1 ("La Campana")	1645	Soybean plot [d]	2376	10000	1762	250	138 (Soybean growth period)
Plot 2	1855		2230		1081		
Plot 3	1877		2230		1124		
Plot 4	1893		2250		1297		
Plot 5	15[illegible]2		2250		1069		
Plot 6	1541		2250		1055		
Plot 7	1500		2250		1219		
Plot 8	1523		2171		1315		
Plot 9	1653		2200		1420		
Average	1670		2245		1260		
RMSE (m^3 t^{-1})			597		494		

Bias (m^3 t^{-1})			575		-410		

CWU was estimated by applying the following ET_{green} calculation equations:

[a] $ET_{green} = EF_{(wl\ or\ wb)}\ (1.46\ NDVI - 0.17) ET_o$. In plot 1, EF is calculated with a weighing lysimeter. In the other plots, a soil water balance was conducted using the CROPWAT model.

[b] $\mathrm{ET}_{green} = \mathrm{K}_s\ \mathrm{K}_c\ ET_o$

[c] $\mathrm{ET}_{green} = (1 - \mathrm{TDVI})\ (1.46\ \mathrm{NDVI} - 0.17)\ ET_o$

[d] Average plot area 80 ha

Credit Author Statement

P. Olivera Rodriguez: conceptualization, methodology, validation, investigation, writing-original draft, review and editing, visualization.

M. E. Holzman: conceptualization, methodology, writing-original draft, review and editing.

M. F. Degano: conceptualization.

A. M. G. Faramiñán: formal analysis.

R. E. Rivas: conceptualization, methodology, writing-original draft.

M. I. Bayala: validation, formal analysis.

Graphical abstract

HIGHLIGHTS

- The estimation of the Green Water Footprint can be optimized using satellite data
- Spatial variability was obtained using evaporative fraction and yield data
- The technique allows the calculation of Green Water Footprint at regional scale
- It can be a contribution to previous methods for agricultural water use estimation